Preprints, 4th IFAC Conference on
Advances in Proportional-Integral-Derivative Control
Almería, Spain | June 12-14, 2024

Resilient Frequency-shifted IMC-PID Scheme for Mitigating Scaling and Random Attacks in Thermal Plants Amid Delay

Pulakraj Aryan * **Nikhil Kumar** ** **G. Lloyds Raja** ***
Montse Meneses **** **Ramon Vilanova** ****

* *Center for Sustainable Energy, Indian Institute of Technology, Roorkee 247667, India.*
** *ALSTOM, Bengaluru, India*
*** *Electrical Engineering Department, National Institute of Technology, Patna 800005, India (e-mail: lloyd.raja@gmail.com)*
**** *Department of Telecommunications and Systems Engineering, Autonomous University of Barcelona, Barcelona, Spain (e-mail: Ramon.Vilanova@uab.cat)*

Abstract: In recent times, several network-related scenarios like Communication Delays (CDs) and malicious Cyber Attacks (CAs) have posed a major challenge in keeping the operational frequency of automatic generation systems within admissible levels. Hence, the proposed work focuses on investigating the applicability of an Frequency-Shifted Internal Model Control-Proportional Integral Derivative (FIMC-PID) controller for Load Frequency Control (LFC) of a non-identical dual-area Power System (PS) in the presence of inherent CDs and CAs. The FIMC approach is based on the integration of concepts like model order reduction and pole-zero shifting of the reduced order transfer function by the constant (ψ) which indicates the amount by which system robustness can be manipulated. In addition to that, an analytical approach for obtaining a stable numerical range of the tunable parameter ψ is introduced using Routh-Hurwitz criteria. This range serves as the input for the Golden Jackal Optimizer (GJO) for finding the optimal value of ψ by minimizing the Integrated Time-Squared Error (ITSE). False Data Injection (FDI) threats to the cyber-physical systems like scaling and random attacks have been modeled and the efficacy of GJO-tuned FIMC strategy in mitigating the same is vindicated. Finally, hardware-in-loop real-time verification of the suggested strategy in mitigating frequency fluctuations is carried out in the OPAL-RT platform.

Keywords: Load frequency Control, Frequency-shifted Internal Model Control, Golden Jackal Optimizer, Cyber-attacks, Communication delay, Robustness.

1. INTRODUCTION

Load Frequency Control (LFC) is the preservation of system frequency and regulation of tie-line interchange schedules amid changing load demands occurring in interconnected Power Systems (PSs). LFC in modern power systems have to handle real-time uncertainties associated with network-induced threats like Cyber Attacks (CAs) and Communication Delays (CDs) (Ram Babu et al. (2022)). Traditionally, Integral (I), Proportional-Integral (PI), and Proportional-Integral-Derivative (PID) controllers were used for LFC applications (Shankar et al. (2017)). These conventional controllers fail to handle uncertainties and disturbance mitigation effectively due to design limitations. To overcome the sluggishness in performance, control techniques like fractional order (FO) controllers, cascaded controllers Ansari and Raja (2024), Fuzzy Logic-based Controllers (FLC) (Kumari et al. (2023), Anand et al. (2022)) give a better dynamic response in LFC application. In the context of LFC, several advanced controllers have been theorized in the past viz Model Predictive Controller (MPC) (Zhu et al. (2022)) and Linear Active Disturbance Rejection Control(L-ADRC) (Sharma et al. (2021)). However, PID controllers are preferable in industries due to their simplicity and feasibility of practical implementation compared to other advanced/complex controllers (Shamsuzzoha and Raja (2023), Mehta et al. (2023)).

Analytical internal model control (IMC)-based PID designs for LFC have received much attention in recent times (Saxena and Hote (2017),Kumar and Hote (2020)). Kumar and Hote (2020) have used an IMC-based PID with Double-derivative (PIDD2) strategy tuned for desired maximum sensitivity. However, the majority of the aforementioned methods rely on hit and trial searches to find suitable tuning parameter values. Some recent studies on industrial process control have vindicated the effectiveness of choosing the adjustable parameters in analytically-

⋆ This work has received support from the Catalan Government under Project 2021 SGR 00197 and also by the Spanish Government under MICINN project PID2019-105434RBC33 co-funded with the European Union ERDF funds.

designed controllers using such metaheuristic optimizers (Aryan and Raja (2022b),Aryan and Raja (2022a),Aryan and Raja (2022c)) to obtain optimally tuned values for adjustable parameters.

The prevalence of CAs and CDs leads to disruption in the safe and secure operation of interconnected Cyber-physical Systems (CPS) (Zhang et al. (2022)). Hence, the impact of CDs has been studied in recent works of LFC considering various PS configurations (Kumar and Hote (2020),Zhao et al. (2022),Raouf and Mousavian (2023)). Likewise, the impact of CAs like Denial-of-service (DoS) and False Data Injection (FDI) have also received considerable research attention in recent times (Yan et al. (2022),Kumar (2022),ShangGuan et al. (2021),Zhang et al. (2022)). However, very little literature focus on studying the impact of both CDs and CAs simultaneously which is a challenging problem in CPS (Kumar (2022),Zhang et al. (2022), Kumar et al. (2023)). Also, it is worth combining the advantages of metaheuristic approaches with analytical controller design strategies to tackle CAs and CDs for effective LFC.

Aryan et al. (2023) have reported a robust frequency-shifted IMC (FIMC) design that involves a pole-zero re-located model. The FIMC-based design has shown significant enhancement in performance and robustness over IMC-based designs. However, this FIMC method is yet to be extended for non-identical dual-area PSs with inherent CDs. Moreover, the single tuning parameter of FIMC (ψ) had to be selected within a given range using the hit-and-trial approach (Aryan et al. (2023)). Golden Jackal Optimizer (GJO) which was reported by Chopra and Ansari (2022) has shown enhanced convergence characteristics than its contemporaries. It is worth augmenting the FIMC method (for PID design) with GJO (for selection of optimal frequency-shifting parameter) to develop an effective LFC strategy to mitigate CDs and CAs.

Motivated by the above observations, the current work aims at accomplishing the following in a dual-area non-identical thermal-thermal interconnected PS:

(1) To re-design PID controllers using the FIMC approach for both control areas as a function of the frequency-shifting parameter (ψ) both with and without CD.
(2) To obtain the stable analytically-obtained range of ψ using Routh-Hurwitz (RH) criteria for both control areas.
(3) To perform an optimal search of ψ within the aforesaid range using GJO by minimization of Integrated Time-squared Error (ITSE).
(4) To model scaling and random type CAs amid CD for elucidating the robustness of the GJO-tuned FIMC controller in mitigating the same.
(5) To perform a real-time verification of the GJO-tuned FIMC-PID control-strategy.

In section 2, the PS configuration is explained and CA models are detailed. Section 3 deliberates controller design steps. An overview of GJO is propounded in Section 4. Section 5 contains simulation results and related discussions. Finally, concluding remarks are reported in Section 6.

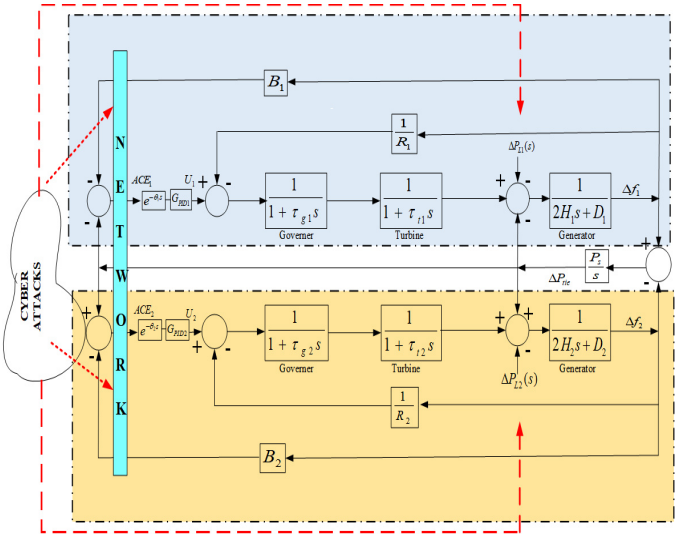

Fig. 1. Dual-area CPS non-identical non-reheat type thermal PS.

2. THEORETICAL FORMULATIONS

2.1 Power system description

Dual-area non-reheated interconnected thermal power plant with non-identical parameters is taken into account. The individual base power rating of both areas is 1000 MVA. Both units are simultaneously under operation at a nominal frequency of 60 Hz. These initial operating conditions are used to calculate the synchronizing power coefficient as $P_s = 2.0$ per unit (p.u.) (Kumar et al. (2023)). Both areas have internal operating units like speed governor with non-reheated steam turbine and generation units whose mathematical models are depicted in Fig. 1.

In Fig. 1, B_1 and B_2 are frequency-bias parameters. Area control errors are denoted by ACE_1 and ACE_2. R_1 and R_2 are speed-regulation constants of respective governors. T_{g1} and T_{g2} are time constants of governors whereas τ_{t1} and τ_{t2} are respective time constants of turbines. D_1 and D_2 are frequency-sensing load coefficients. Inertia constants are denoted by H_1 and H_2. The dynamics of various blocks of PS in i_{th} area are as follows:

$$G_{Governer,i}(s) = \frac{1}{1+\tau_{gi}s} \tag{1}$$

$$G_{Turbine,i}(s) = \frac{1}{1+\tau_{ti}s} \tag{2}$$

$$G_{Generator,i}(s) = \frac{1}{2H_is+D_i} \tag{3}$$

From Fig. 1, we get

$$\Delta f_i(s) = G_{si}(s)U_i(s) + G_{Di}(s)\Delta P_{Li} \tag{4}$$

where, Δf_i is the frequency deviation, $U_i(s)$ is the output of the controller and ΔP_{Li} is the disturbance. Since LFC is a disturbance mitigation problem, the motive is to stabilize G_{si} under the influence of ΔP_{Li} while mitigating the effect of ΔP_{Li} on Δf_i using control action. ACE_i, ΔP_{tie} (tie-line power deviation) and Δf_i are related as

$$ACE_i = B_i\Delta f_i + \Delta P_{tie} \tag{5}$$

where B_i is the frequency bias coefficient. The ACE serves as the input to the controller. The open-loop transfer function $G_{OLTF}(s)$ for an i_{th} area without droop characteristics is calculated as follows:

$$G_{OLTF,i}(s) = G_{Goverer,i}(s)G_{Turbine,i}(s)G_{Generator,i}(s) \quad (6)$$

The closed-loop plant model $G_{Si}(s)$ (from a servo perspective) for i_{th} area is obtained as

$$G_{si}(s) = B_i \frac{G_{OLTF,i}(s)}{1 + G_{OLTF,i}(s)/R_i} \quad (7)$$

Using (1)-(3) in (7), we get

$$G_{si}(s) = B_i \frac{\frac{1}{(1+s\tau_{gi})(1+s\tau_{ti})(2H_i s+D_i)}}{1 + \frac{1}{(1+s\tau_{gi})(1+s\tau_{ti})(2H_i s+D_i)R_i}} \quad (8)$$

Rearranging (8) yields

$$G_{si}(s) = \frac{R_i B_i}{R_i(1+s\tau_{gi})(1+s\tau_{ti})(2H_i s + D_i) + 1} \quad (9)$$

The above equation is of the form

$$G_{si}(s) = \frac{B_i/A}{s^3 + (B/A)s^2 + (C/A)s + (D/A)} \quad (10)$$

where

$$\begin{aligned} A &= 2H_i\tau_{gi}\tau_{ti} \\ B &= (2H_i\tau_{gi} + 2H_i\tau_{ti} + D_i\tau_{ti}\tau_{gi}) \\ C &= (2H_i + D_i\tau_{ti} + D_i\tau_{gi}) \\ D &= D_i + 1/R_i \end{aligned} \quad (11)$$

For area-1, the PS parameters are as follows: R_1 = 0.05Hz/p.u.MW, $D_1 = 0.6$, $H_1 = 5s$, $B_1 = 20.6$ p.uMW/Hz, Base power = 1000MVA, $\tau_{g1} = 0.2s$, $\tau_{t1} = 0.5s$. In the case of area-2, the PS parameters are as follows: $R_2 = 0.0625$Hz/p.u.MW, $D_2 = 0.9$, $H_2 = 4s$, $B_2 =$ 1p.u.MW/Hz, Base power = 1000MVA, $\tau_{g2} = 0.3s$, $\tau_{t2} = 0.6s$ (Kumar et al. (2023)) At the nominal frequency of 60 Hz, the units are running parallel. The initial operating parameters are used to calculate the synchronizing power coefficient, which is given as $P_S = 2.0$p.u(MW/radian).

The model order reduction technique is used for appoximating a higher-order system with a lower-order transfer function so that simple controllers can be designed using the same. The fundamental idea is to keep the dominant poles of the plant model while rejecting the non-dominant poles. The Pade-based model-order reduction strategy adopted in this work relies on equating a small number of Taylor series coefficients at $s = 0$ from the reduced-order model to the equivalent coefficients from the original model. Accordingly, a second-order reduced model of i_{th} area thermal PS is obtained as follows:

$$R_{si}(s) = \frac{a_0 - a_1 s}{b_0 + b_1 s + s^2} \quad (12)$$

2.2 Cyber-attacks

The model projected in Fig. 1 is treated as a CPS where there is the application of sensing, communication, and computer technology. The vulnerable points where attackers can gain access are highlighted using arrows in Fig. 1. To corroborate the robustness of the FIMC controller against such unprecedented scenarios, various attack models have been considered in the literature (Ghiasi et al. (2023)). Two such models are discussed below:

Scaling attack This is a different version of template attack such that the error signal amplitude is scaled before it is fed to the controller. The magnitude of the error signal is either incremented or decremented as per the attack strategy during the transient phase. This attack signal $ACE_u^*(t)$ is mathematically expressed as follows:

$$ACE_u^*(t) = \begin{cases} a(\beta_i \Delta f_i(t) + \Delta P_{tie}(t)) \ \forall \ t \in \tau_a \\ \beta_i \Delta f_i(t) + \Delta P_{tie}(t) \ \forall \ t \notin \tau_a \end{cases} \quad (13)$$

where a is the error scaling factor. τ_a denotes the attack duration. Other symbols in the above equation have their usual meanings as stated in (5). This attack falsifies the magnitude of ACE for the attack duration causing transmission of the corrupted control signal to the plant.

Random attack Error signals of random nature are fed through the channel in this sort of attack thus initiates control action when it is not supposed to happen. It lets the transmission signals through the communication channel go completely in haywire mode leading to the deterioration of dynamic performance. This attack signal $ACE_u^*(t)$ is mathematically expressed as

$$ACE_u^*(t) = \begin{cases} f_g(x) \forall t \in \tau_a \\ \beta_i \Delta f_i(t) + \Delta P_{tie}(t) \forall t \notin \tau_a \end{cases} \quad (14)$$

During the attack execution, the normal incoming feedback signal through the ACE channel is blocked and a signal $f_g(x) = \frac{1}{\sigma\sqrt{2\pi}} e^{\frac{-(x-\mu)^2}{2\sigma^2}}$ where μ = mean of the distribution and σ = standard deviation and τ_a is attack duration. Other symbols in the above equation have their usual meanings as stated in (5). $f_g(x)$ is of gaussian nature. As false data is transmitted through the channel to the controller which results in arbitrary control commands leading to the fluctuation in frequency and tie-line power.

3. FREQUENCY-SHIFTED IMC-PID DESIGN

Due to the filter involved in IMC-PID design (Saxena and Hote (2013)), additional phase lag is introduced. Hence, the traditional IMC design procedure must be modified such that the performance and robustness can be strengthened. Especially, while dealing with LFC problems amid real-time challenges like CDs, CAs, and parametric uncertainties, a robust IMC strategy is vital. The FIMC design does not involve an IMC filter (Aryan et al. (2023)) and if a controller $Q(s)$ is designed using a frequency-shifted version of the plant model $G_M(s - \psi)$ instead of $G_M(s)$, then robustness of $Q(s)$ can be adjusted by varying ψ. In other words, a control-loop designed using $G_M(s - \psi)$ will be less sensitive to parametric aberrations (more robust) than that designed using $G_M(s)$, $\forall \psi < 0$ (Aryan et al. (2023)). Efficient FIMC-PID design requires a robust and stable operating range for ψ. This range serves as input to GJO yielding an optimal FIMC-PID controller with a satisfactory performance-robustness trade-off. The frequency shifted version of (12) is

$$R_{si}(s - \Psi) = \frac{-a_1(s - \Psi) + a_0}{b_0 + b_1(s - \Psi) + (s - \Psi)^2} \quad (15)$$

Splitting (15) into invertible and non-invertible components yields

$$R_{si}(s-\Psi) = R_{si-}(s-\Psi)R_{si+}(s-\Psi) \tag{16}$$

where

$$\left.\begin{aligned} R_{si-}(s-\Psi) &= \left(\frac{a_1 s + a_1\Psi + a_0}{b_0 + b_1(s-\Psi) + (s-\Psi)^2}\right) \\ R_{si+}(s-\Psi) &= \left(\frac{-a_1 s + a_1\Psi + a_0}{a_1 s + a_1\Psi + a_0}\right) \end{aligned}\right\} \tag{17}$$

The idealized FIMC controller is given by

$$Q(s) = \frac{1}{R_{si-}(s-\Psi)} \tag{18}$$

$$Q(s) = \frac{b_0 + b_1(s-\Psi) + (s-\Psi)^2}{a_1 s + a_1\Psi + a_0} \tag{19}$$

Equation (19) can be expressed in realisable form as follows:

$$G_{PID} = \frac{Q(s)}{1 - Q(s)R_{si}(s-\Psi)} \tag{20}$$

$$= \frac{\frac{b_0+b_1(s-\Psi)+(s-\Psi)^2}{a_1 s+a_1\Psi+a_0}}{1 - \left(\frac{b_0+b_1(s-\Psi)+(s-\Psi)^2}{a_1 s+a_1\Psi+a_0}\right)\left(\frac{-a_1(s-\Psi)+a_0}{b_0+b_1(s-\Psi)+(s-\Psi)^2}\right)} \tag{21}$$

Re-arranging (21) results in the following PID form:

$$G_{PID} = K_p + \frac{K_i}{s} + K_d s \tag{22}$$

where

$$K_p = \frac{b_1 - 2\Psi}{2a_1}, K_i = \frac{\Psi^2 - b_1\Psi + b_0}{2a_1}, K_d = \frac{1}{2a_1} \tag{23}$$

PID settings derived in (23) are a function of Ψ. Hence, a stable analytical range of Ψ has to be obtained for both areas using RH criteria. Using (10), (11) and (22), the closed-loop characteristic equation is obtained as follows:

$$1 + G_{si}(s)G_{PIDi}(s) = 0 \tag{24}$$

where

$$1 + \left(\frac{B_i}{As^3 + Bs^2 + Cs + D}\right)\left(K_p + \frac{K_i}{s} + K_d s\right) = 0 \tag{25}$$

Rearranging (25) as a polynomial yield

$$As^4 + Bs^3 + (B_iK_d + C)s^2 + (B_iK_p + D)s + B_iK_i = 0 \tag{26}$$

Using RH criteria, we obtain the following:

$$B_iK_i > 0 \tag{27}$$

$$BB_iK_d + BC - AB_iK_p - AD > 0 \tag{28}$$

$$\begin{pmatrix} BCD + K_P BCB_i + BDB_iK_d + K_pBB_i^2K_d \\ -A(B_i^2{K_P}^2 + D^2 + 2B_iK_pD) - B^2B_iK_i \end{pmatrix} > 0 \tag{29}$$

where expressions of A, B, C, and D are given in (11). Substituting the PS parameters in (27)-(29) yields $-2.109 < \Psi < 0.778$ (for area-1) and $-1.385 < \Psi < 0.57$ (for area-2).

3.1 Controller design amid communication delay

In this case, a delay term is considered in (12) as follows:

$$R_{si\theta}(s) = \frac{-a_1 s + a_0}{b_0 + b_1 s + s^2} e^{-\theta s} \tag{30}$$

Rearranging numerator of (30) yields

$$R_{si\theta}(s) = \frac{a_0\left(1 - \frac{a_1}{a_0}s\right)e^{-\theta s}}{b_0 + b_1 s + s^2} \tag{31}$$

The numerator term $1 - \left(\frac{a_1}{a_0}\right)s$ of (30) is approximated as a delay-term $e^{\left(\frac{-a_1}{a_0}\right)s} = 1 - \left(\frac{a_1}{a_0}\right)s$ using Taylor series approximation to get

$$R_{si\theta}(s) = \frac{a_0 e^{-\theta s} e^{-\left(\frac{a_1}{a_0}\right)s}}{b_0 + b_1 s + s^2} \tag{32}$$

Using the FIMC-PID design approach, we get the following settings:

$$\left.\begin{aligned} K_p &= \frac{b_1 - 2\Psi}{2a_0\left(\theta + \frac{a_1}{a_0}\right)}, \\ K_i &= \frac{\Psi^2 - b_1\Psi + b_0}{2a_0\left(\theta + \frac{a_1}{a_0}\right)}, \\ K_d &= \frac{1}{2a_0\left(\theta + \frac{a_1}{a_0}\right)} \end{aligned}\right\} \tag{33}$$

4. GOLDEN JACKAL OPTIMIZER

GJO (Chopra and Ansari (2022)), a nature-inspired optimization technique mimics the hunting pattern of a golden jackal. GJO has reportedly shown better fitness characteristics compared to its contemporaries like particle swarm optimizer, African vultures optimizer, Arithmetic optimizer and equilibrium optimizer. Hence, GJO is used to tune Ψ such that the following objective function is minimized:

$$J_{ITSE} = \int_0^T \left[ACE_1^2 + ACE_2^2\right]tdt \tag{34}$$

where, ACE_1 and ACE_2 are area control errors. T is the simulation time. The detailed steps of GJO are summarized in (Kumar et al. (2023)).

5. RESULTS AND DISCUSSION

All simulations in this section are performed using MATLAB and Simulink on an Intel Core i3 processor. Transfer functions described in (1),(2) and (3) are used to construct the block diagram in Fig. 1. Values of PS parameters are given in Section 2.

5.1 Dynamic responses amid communication delay

A robust counter-delay strategy is vital for effective LFC such that control signals can be received without any time lag. Hence, an inherent communication delay of θ

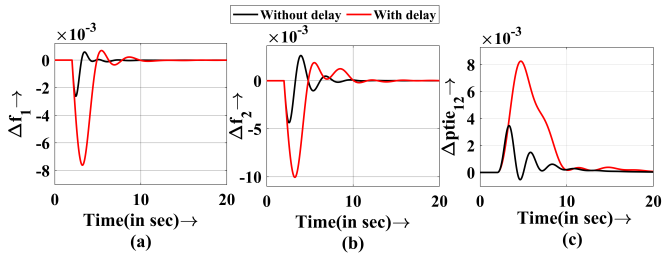

Fig. 2. Effect of communication delay on dynamic responses (a) Frequency deflection in area-1, (b) Frequency deflection in area-2, and (c) Tie-line power deflection

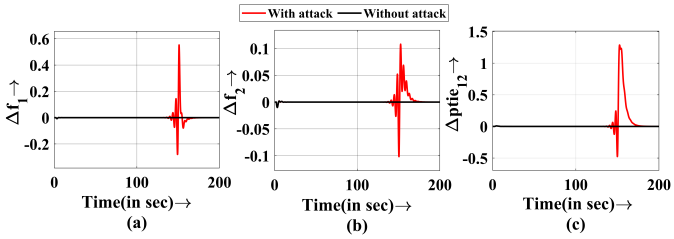

Fig. 3. Responses for template attack (a) Frequency deflection in area-1 (b) Frequency deflection in area-2 (c) Tie-line power deflection

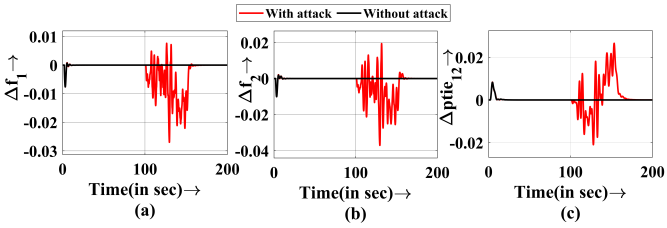

Fig. 4. Responses for random attack (a) Frequency deflection in area-1 (b) Frequency deflection in area-2 (c) Tie-line power deflection

sec is considered in the present design. The respective controller settings are obtained using (33). For $\theta = 1$ sec, the range of Ψ obtained using RH criteria are as follows: $-0.289 < \Psi < 1.864$ (for area-1) and $-0.619 < \Psi < 1.644$ (for area-2). The FIMC-PID settings are as follows: $K_p = 0.1754, K_i = 0.4470, K_d = 0.1470$ (for area-1) and $K_p = 0.0210, K_i = 0.4061, K_d = 0.1760$ (for area-2). A load disruption $\Delta P_{Li} = 0.1$ p.u is introduced to the test system at $t = 2s$ in both areas. The controller could handle the considered delay and the response settles at zero frequency-deviation baselines as demonstrated in Fig. 2.

5.2 Cyber-attack simulation

This part demonstrates the impact of attacks described in Section 2 on the performance of the GJO-tuned FIMC-PID strategy. An inherent delay in the LFC loop is taken as $\theta = 1s$. In both the attacks discussed in this subsection, the actual signal is blocked for a while false data is fed into specified locations of the CPS (marked in Fig. 1). Note that the course for which the simulation run is taken to be $200s$ for each attack.

Fig. 5. OPAL-RT based HIL setup

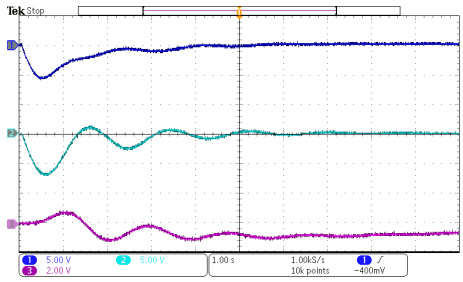

Fig. 6. Results of real-time validation: (1) frequency deflection in area-1(2) frequency deflection in area-2 (3) Tie-line power deviation

Scaling/template attack A scaling attack is a type of template attack in which the ACE value is scaled up a-times by the attacker for a certain duration. For $a = 5$, $(100s < \tau_a < 150s)$. Equation (13) is used to simulate a scaling attack. As a result of the above attack, the response becomes oscillatory with high magnitude for a while before they are mitigated by the GJO-tuned FIMC strategy as evident from Fig. 3. Thus the resilience of the controller towards scaling attacks is vindicated.

Random attack The random attack is simulated using a Gaussian-distributed random signal with $\mu = 0$, $\sigma = 0.316$ (using (14)) to supply some random values when the actual ACE signal is blocked for a specific attack duration $(100s < \tau_a < 150s)$. Fig. 4 vindicates that the proposed controller is resilient towards random attacks.

5.3 Real-time verification

This subsection presents the results of the real-time simulation that was completely integrated with the MATLAB 2020a/simulink environment. The OPAL-RT OP5700 FPGA-based simulator (Fig. 5) is used for verifying the simulation findings. A prototype model shown in Fig. 1 is taken up for simulation with a considerable delay of 1 sec in the LFC system. The model is loaded and executed using compatible software. It is clear from Fig. 6 that it is an exact reproduction of what has been obtained using MATLAB Simulink in Fig. 2. Thus the practical feasibility of the proposed controller technique is evident.

6. CONCLUSION

In this work, the resiliency of the frequency-shifted indirect internal model control (FIMC) based proportional-integral-derivative (PID) controller tuned with Golden Jackal Optimizer (GJO) in dealing with scaling and random attacks is demonstrated using a benchmark non-identical dual-area thermal power system. For this pur-

pose, the scaling and random attack signals are modeled and injected into the load frequency control loop by temporarily blocking the actual signal. Simulation studies show that the GJO-tuned FIMC-PID design yields satisfactory resilience in mitigating the false data injection attacks amid siginificant communication delay. Real-time validation of the FIMC-PID design is carried out to vindicate its practical feasibility.

REFERENCES

Anand, A., Aryan, P., Kumari, N., and Raja, G.L. (2022). Type-2 fuzzy-based branched controller tuned using arithmetic optimizer for load frequency control. *Energy Sources, Part A: Recovery, Utilization, and Environmental Effects*, 44(2), 4575–4596.

Ansari, Z.A. and Raja, G.L. (2024). Flow direction optimizer tuned robust fopid-(1+ td) cascade controller for oscillation mitigation in multi-area renewable integrated hybrid power system with hybrid electrical energy storage. *Journal of Energy Storage*, 83, 110616.

Aryan, P. and Raja, G.L. (2022a). Design and analysis of novel qoeo optimized parallel fuzzy fopi-pidn controller for restructured agc with hvdc and pev. *Iranian Journal of Science and Technology, Transactions of Electrical Engineering*, 46(2), 565–587.

Aryan, P. and Raja, G.L. (2022b). A novel equilibrium optimized double-loop control scheme for unstable and integrating chemical processes involving dead time. *International Journal of Chemical Reactor Engineering*, 20(12), 1341–1360.

Aryan, P. and Raja, G.L. (2022c). Restructured lfc scheme with renewables and ev penetration using novel qoea optimized parallel fuzzy i-pid controller. *IFAC-PapersOnLine*, 55(1), 460–466.

Aryan, P., Raja, G.L., Vilanova, R., and Meneses, M. (2023). Repositioned internal model control strategy on time-delayed industrial processes with inverse behavior using equilibrium optimizer. *IEEE Access*.

Chopra, N. and Ansari, M.M. (2022). Golden jackal optimization: A novel nature-inspired optimizer for engineering applications. *Expert Systems with Applications*, 198, 116924.

Ghiasi, M., Niknam, T., Wang, Z., Mehrandezh, M., Dehghani, M., and Ghadimi, N. (2023). A comprehensive review of cyber-attacks and defense mechanisms for improving security in smart grid energy systems: Past, present and future. *Electric Power Systems Research*, 215, 108975.

Kumar, M. (2022). Resilient pida control design based frequency regulation of interconnected time-delayed microgrid under cyber-attacks. *IEEE Transactions on Industry Applications*.

Kumar, M. and Hote, Y.V. (2020). Robust pidd2 controller design for perturbed load frequency control of an interconnected time-delayed power systems. *IEEE Transactions on Control Systems Technology*, 29(6), 2662–2669.

Kumar, N., Aryan, P., Raja, G.L., and Muduli, U.R. (2023). Robust frequency-shifting based control amid false data injection attacks for interconnected power systems with communication delay. *IEEE Transactions on Industry Applications*, 1–14. doi: 10.1109/TIA.2023.3348775.

Kumari, N., Aryan, P., Raja, G.L., and Arya, Y. (2023). Dual degree branched type-2 fuzzy controller optimized with a hybrid algorithm for frequency regulation in a triple-area power system integrated with renewable sources. *Protection and Control of Modern Power Systems*, 8(3), 1–29.

Mehta, U., Aryan, P., and Raja, G.L. (2023). Tri-parametric fractional-order controller design for integrating systems with time delay. *IEEE Transactions on Circuits and Systems II: Express Briefs*.

Ram Babu, N., Bhagat, S.K., Saikia, L.C., Chiranjeevi, T., Devarapalli, R., and García Márquez, F.P. (2022). A comprehensive review of recent strategies on automatic generation control/load frequency control in power systems. *Archives of Computational Methods in Engineering*, 1–30.

Raouf, B. and Mousavian, S. (2023). A robust controller design based on kharitonov's theorem for frequency control in an interconnected power system. *European Journal of Electrical Engineering and Computer Science*, 7(1), 1–9.

Saxena, S. and Hote, Y.V. (2013). Load frequency control in power systems via internal model control scheme and model-order reduction. *IEEE transactions on power systems*, 28(3), 2749–2757.

Saxena, S. and Hote, Y.V. (2017). Stabilization of perturbed system via imc: An application to load frequency control. *Control Engineering Practice*, 64, 61–73.

Shamsuzzoha, M. and Raja, G.L. (2023). Pid control for linear and nonlinear industrial processes.

ShangGuan, X.C., He, Y., Zhang, C.K., Jin, L., Jiang, L., Wu, M., and Spencer, J.W. (2021). Switching system-based load frequency control for multi-area power system resilient to denial-of-service attacks. *Control Engineering Practice*, 107, 104678.

Shankar, R., Pradhan, S., Chatterjee, K., and Mandal, R. (2017). A comprehensive state of the art literature survey on lfc mechanism for power system. *Renewable and Sustainable Energy Reviews*, 76, 1185–1207.

Sharma, P., Mishra, A., Saxena, A., and Shankar, R. (2021). A novel hybridized fuzzy pi-ladrc based improved frequency regulation for restructured power system integrating renewable energy and electric vehicles. *IEEE Access*, 9, 7597–7617.

Yan, S., Gu, Z., Park, J.H., Xie, X., and Dou, C. (2022). Probability-density-dependent load frequency control of power systems with random delays and cyber-attacks via circuital implementation. *IEEE Transactions on Smart Grid*, 13(6), 4837–4847.

Zhang, G., Li, J., Bamisile, O., Xing, Y., Cai, D., and Huang, Q. (2022). An h load frequency control scheme for multi-area power system under cyber-attacks and time-varying delays. *IEEE Transactions on Power Systems*.

Zhao, X., Ma, Z., Li, S., and Zou, S. (2022). Robust lfc of power systems with wind power under packet losses and communication delays. *IEEE Journal on Emerging and Selected Topics in Circuits and Systems*, 12(1), 135–148.

Zhu, J., Cui, X., and Ni, W. (2022). Model predictive control based control strategy for battery energy storage system integrated power plant meeting deep load peak shaving demand. *Journal of Energy Storage*, 46, 103811.